

Supplemental Information

Intrathecal bone marrow stromal cells inhibit neuropathic pain via TGF- β secretion

Gang Chen, Chul-Kyu Park, Rou-Gang Xie, and Ru-Rong Ji

Supplemental Methods

Supplemental Table: 2

Supplemental Figures: 8

Supplemental Methods

BMSCs Culture and Flow Cytometry Analysis.

Primary cultures of BMSCs were obtained from CD-1 donor mice under aseptic conditions. The mice were sacrificed with isoflurane and the both ends of the tibiae and femurs were cut off by scissors. A syringe fitted with 20-gauge needle was inserted into the shaft of the bone, and bone marrow was flushed out with culture medium (modified Eagle's medium containing 10% fetal bovine serum, 2mM L-glutamine, 100 U/mL penicillin and 100 µg/mL streptomycin, 250 µg/mL Fungizone, all obtained from Gibco). After the centrifuge at 1000g for 5 min at room temperature, the pellet was resuspended in 2 ml fresh warm culture medium and mechanically dissociated, and the suspension was passed through a 40-µm cell strainer to remove debris. After the centrifuge the cells were resuspended at a concentration of 1×10^6 cells/ml. The cells were then incubated at 37°C in 5% CO₂ in 75 cm² cell culture flasks or 6-well culture plates. After 24 hours, cells were washed gently with PBS and replaced with fresh culture media. Adherent cells were further cultured with a medium change every 2-3 days until confluence was reached (also see Supplemental Figure 1).

The property of expanded cells was assessed by flow cytometry. The adherent cells were then harvested by incubation with 0.25% trypsin/1 mM EDTA, washed with PBS and counted by the hemocytometer. A single cell suspension of 1×10^6 cells was placed in 0.05 ml of staining buffer (eBioscience). The cells were incubated with saturating concentrations of fluorescein isothiocyanate (FITC)-conjugated monoclonal antibodies against CD45 (1:400, eBioscience) and CD90 (1:400, eBioscience) for 20 minutes on ice in the dark. Isotype matched FITC-conjugated immunoglobulin G antibodies (1:400, eBioscience) were used as controls. Cells were then washed three times with staining buffer, centrifuged at 1000g for 5 minutes, and resuspended in 0.5 ml ice cold staining buffer. Flow cytometry analyses were performed on Becton-Dickinson FACS Vantage Sorter Flow Cytometer (BD Biosciences) and analyzed using FlowJo analysis software (TreeStar).

Immunohistochemistry.

As we reported previously (1), after appropriate survival times, animals were deeply anesthetized with isoflurane and perfused through the ascending aorta with PBS, followed by 4%

paraformaldehyde with 1.5% picric acid in 0.16 M phosphate buffer. After the perfusion, the lumbar spinal cord segments and DRGs were removed and postfixed in the same fixative overnight. Spinal cord sections (30 μm , free-floating) and DRG sections (12 μm) were cut in a cryostat and processed for immunofluorescence as we described previously (1). The sections were first blocked with 2% goat or horse serum for 1 h at room temperature. The sections were then incubated overnight at 4°C with the following primary antibodies: GFAP antibody (mouse, 1:5000; Millipore Bioscience Research Reagents), IBA-1 antibody (rabbit, 1:1000, Wako), CGRP antibody (rabbit, 1:1000, Abcam), ATF3 antibody (rabbit, 1:1000, Santa Cruz), NeuN antibody (mouse, 1:1000, Millipore), and CD90 antibody (rat, 1:200, BD Pharmingen). The sections were then incubated for 1 h at room temperature with cyanine 3 (Cy3)- or FITC-conjugated secondary antibodies (1:400; Jackson ImmunoResearch). Fluorescein labeled GSLI-isolectin B4 (Vector laboratories) was used to perform IB4 staining (5 $\mu\text{g}/\text{ml}$) for 2 h at room temperature. For double immunofluorescence, sections were incubated with a mixture of polyclonal and monoclonal primary antibodies, followed by a mixture of FITC- and Cy3-conjugated secondary antibodies. In some cases DAPI (Vector laboratories) was used to stain cell nucleus. The stained sections were examined with a Nikon fluorescence microscope, and images were captured with a CCD Spot camera. We collected 6 spinal cord or DRG sections from each mouse for quantification. The intensity of fluorescence was analyzed using NIH Image J software. Some sections were also evaluated with a confocal microscope (Zeiss 510 inverted confocal).

References

- [1] Berta,T., Park,C.K., Xu,Z.Z., Xie,R.G., Liu,T., Lu,N., Liu,Y.C., and Ji,R.R. 2014. Extracellular caspase-6 drives murine inflammatory pain via microglial TNF-alpha secretion. *J Clin. Invest* **124**:1173-1186.

Supplemental Table-1: Summary of the published studies showing the effects of BMSCs in mouse, rat, and human pain conditions following local or systemic injection.

Supplemental Table 1

Year	Authors	Pain and disease Models, species	Cell source	Number of cells	Delivery site	Effect on pain
2007	Musolino, et al. [1]	Single nerve constriction, rat	rat	2×10^5	Intraganglionic	Reduction of mechanical and thermal allodynia for 7 days
2007	Klass, et al. [2]	CCI, rat	rat	1×10^7	Intravenous	Reduction of neuropathic pain on day 10
2008	Shibata, et al. [3]	STZ-induced diabetes rat	rat	1×10^6	Injection in the hind limb skeletal muscle	Improvement of hypoalgesia
2009	Abrams, et al. [4]	spinal cord injury, rat	rat	3×10^5	Injury site	Improvement of mechanical allodynia, no effect on thermal hyperalgesia
2010	Siniscalco, et al. [5]	SNI, mouse	human	5×10^4	Lateral cerebral ventricle	Improvement of mechanical allodynia and thermal hyperalgesia for 2-3 weeks
2011	Siniscalco, et al. [6]	SNI, mouse	human	2×10^6	Intravenous	Improvement of mechanical allodynia and thermal hyperalgesia for 3 months
2011	Orozco, et al. [7]	Degenerative disc disease, human	human	$10 \pm 5 \times 10^6$ per disc	Intradiscal Injection	Pain reduction for 3 months Pilot study, 10 patients
2011	Guo, et al. [8]	CCI orofacial pain, tendon injury, rat	rat	$1.5 \times 10^{3-6}$, $1.5 \sim 3.75 \times 10^5$	Intravenous; Injury site	Pain reduction for several months
2011	Naruse, et al. [9]	STZ-induced diabetes, rat	rat	1×10^6	Injection in the hind limb skeletal muscle	Reduction in mechanical hyperalgesia and cold allodynia for 5 weeks
2014	van Buul, et al. [10]	Osteoarthritis, rat	rat	1×10^6 per joint	Intra-articularly injected	Decrease in pain for 4 weeks
2014	Schäfer, et al. [11]	PSNL, rat	rat	1×10^6 , 3 times	Intrathecal	No effects on pain in 21 days
2014	Zhang, et al. [12]	SNL, rat	rat	1×10^5	Intrathecal	Reduction of mechanical allodynia for 2-3 weeks
2015	Pettine, et al. [13]	Degenerative disc disease, human	human	$2-4 \times 10^8$ nucleated cells per disc	Intradiscal Injection	Low back pain decrease for one year Open label pilot study, 26 patients

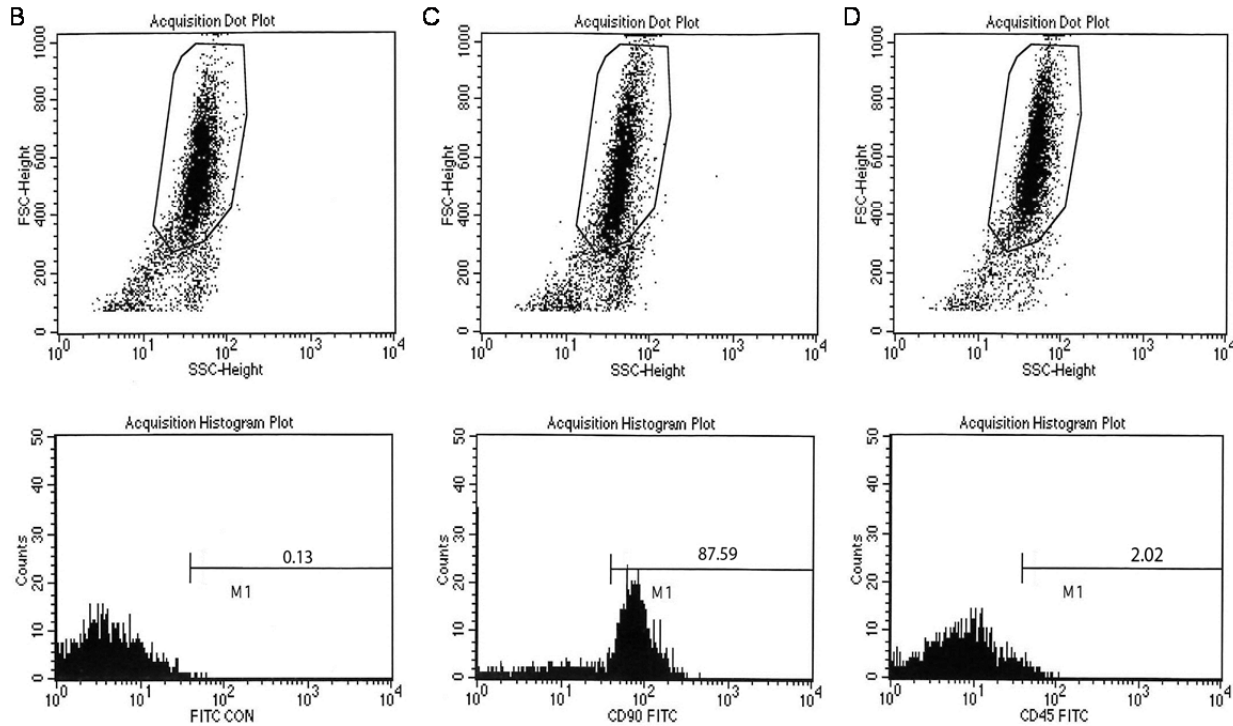
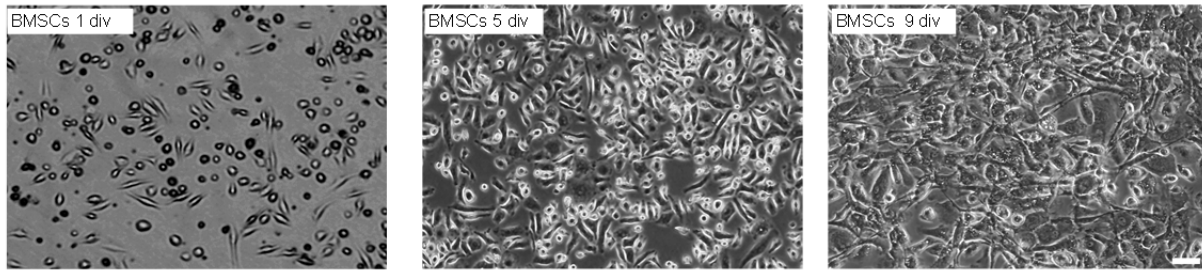
References

- Musolino, P.L., Coronel, M.F., Hokfelt, T., & Villar, M.J. Bone marrow stromal cells induce changes in pain behavior after sciatic nerve constriction. *Neurosci Lett*. **418**, 97-101 (2007).
- Klass, M. et al. Intravenous mononuclear marrow cells reverse neuropathic pain from experimental mononeuropathy. *Anesth Analg*. **104**, 944-948 (2007)
- Shibata, T. et al. Transplantation of bone marrow-derived mesenchymal stem cells improves diabetic polyneuropathy in rats. *Diabetes*. **57**, 3099-3107 (2008)
- Abrams, M. et al. Multipotent mesenchymal stromal cells attenuate chronic inflammation and injury-induced sensitivity to mechanical stimuli in experimental spinal cord injury. *Restor Neurol Neurosci*. **27**, 307-321 (2009)
- Siniscalco, D. et al. Intra-brain microinjection of human mesenchymal stem cells decreases allodynia in neuropathic mice. *Cell Mol Life Sci*. **67**, 655-669 (2010)
- Siniscalco, D. et al. Long-lasting effects of human mesenchymal stem cell systemic administration on pain-like behaviors, cellular, and biomolecular modifications in neuropathic mice. *Front Integr Neurosci* **5**, 79 (2011).
- Orozco, L. et al. Intervertebral disc repair by autologous mesenchymal bone marrow cells: a pilot study. *Transplantation*. **92**, 822-828 (2011)
- Guo, W. et al. Bone marrow stromal cells produce long-term pain relief in rat models of persistent pain. *Stem Cells* **29**, 1294-1303 (2011).
- Naruse, K. et al. Transplantation of bone marrow-derived mononuclear cells improves mechanical hyperalgesia, cold allodynia and nerve function in diabetic neuropathy. *PLoS ONE*. **6**, e27458 (2011).
- van Buul, G.M. et al. Mesenchymal stem cells reduce pain but not degenerative changes in a mono-iodoacetate rat model of osteoarthritis. *J Orthop. Res*. **32**, 1167-1174 (2014).
- Schäfer, S. et al. Influence of intrathecal delivery of bone marrow-derived mesenchymal stem cells on spinal inflammation and pain hypersensitivity in a rat model of peripheral nerve injury. *J Neuroinflammation*. **11**, 157 (2014)
- Zhang, E.J., Song, C.H., Ko, Y.K., and Lee, W.H. Intrathecal administration of mesenchymal stem cells reduces the reactive oxygen species and pain behavior in neuropathic rats. *Korean J Pain*. **27**, 239-245 (2014)
- Pettine, K.A., Murphy, M.B., Suzuki, R.K., and Sand, T.T. Percutaneous injection of autologous bone marrow concentrate cells significantly reduces lumbar discogenic pain through 12 months. *Stem Cells*. **33**, 146-156 (2015)

Supplementary Table 2: Sample size and numbers of mice used in each experiment. A total of 448 mice were used in this study.

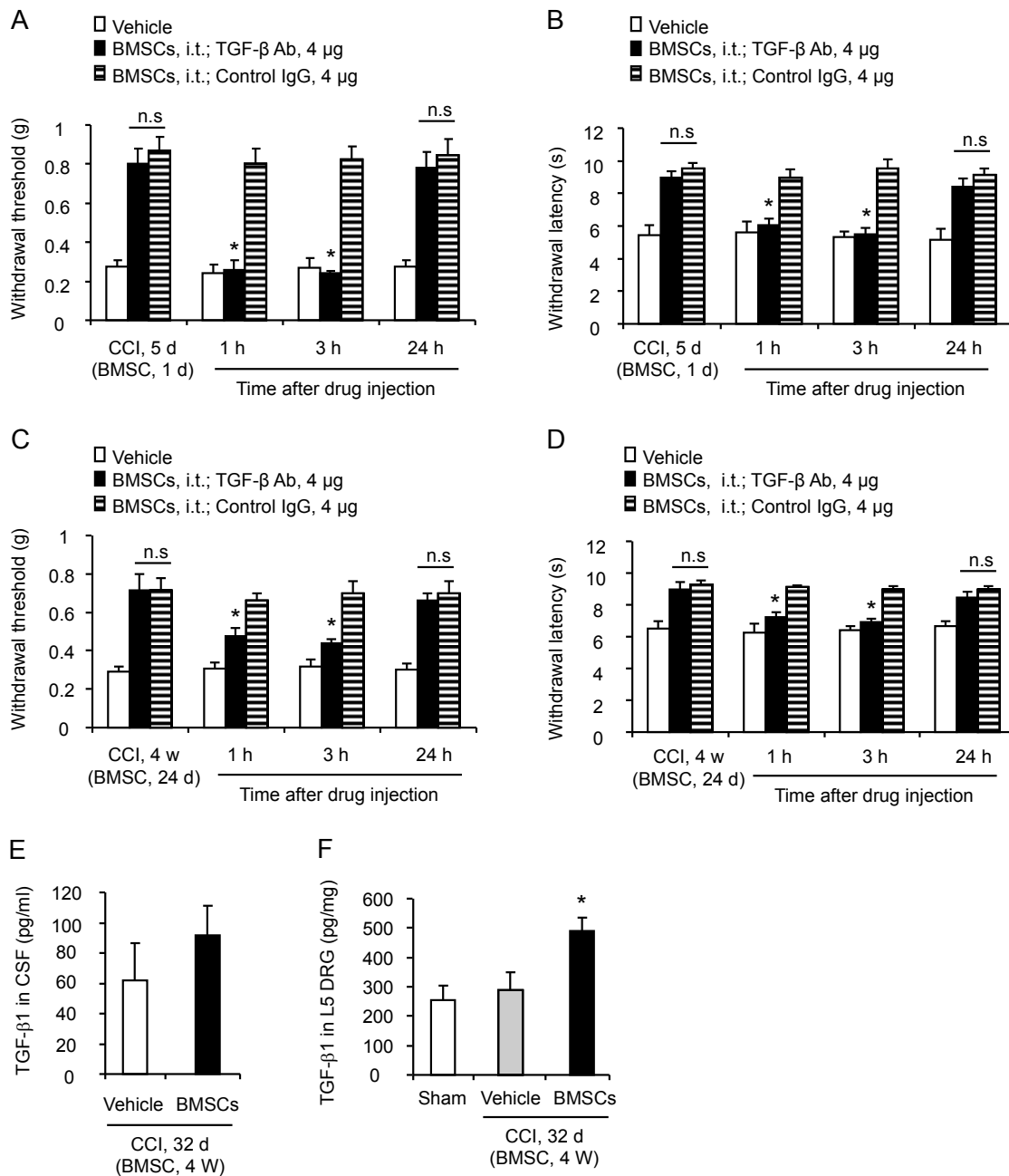
Experiment	Sample size	Number of Groups	Number of samples	Number of mice
1. In vivo				
1.1 Behavioral test	n = 5-6 mice	31	173 mice	173
1.2 RT-PCR	n = 4-5 mice	4	17 mice	17
1.3 CSF Elisa analysis	n = 4 mice	5	20 mice	20
1.4 Elisa for DRG tissues	n = 4 mice	6	24 mice	24
1.5 Immunohistochemistry				
1.5.1 DRG tissues	n = 4-5 mice	12	51 mice	51
1.5.2 Spinal cord tissues	n = 4-5 mice	7	31mice	31
2. Ex vivo				
2.1 Patch-clamp recording	n = 5 neurons	8	40 neurons	22
3. In vitro				
3.1 BMSCs culture				
3.1.1 Flow cytometric analysis	n = 6 cultures	5	30 cultures	15
3.1.2 Elisa	n = 4-8 cultures	8	36 cultures	20
3.1.3 Transwell chemotaxis	n = 4 cultures	5	20 cultures	10
3.1.4 RT-PCR	n = 3 cultures	2	6 cultures	3
3.1.5 Intrathecal injection	n = 125 cultures			62
			Total number of mice	448

A



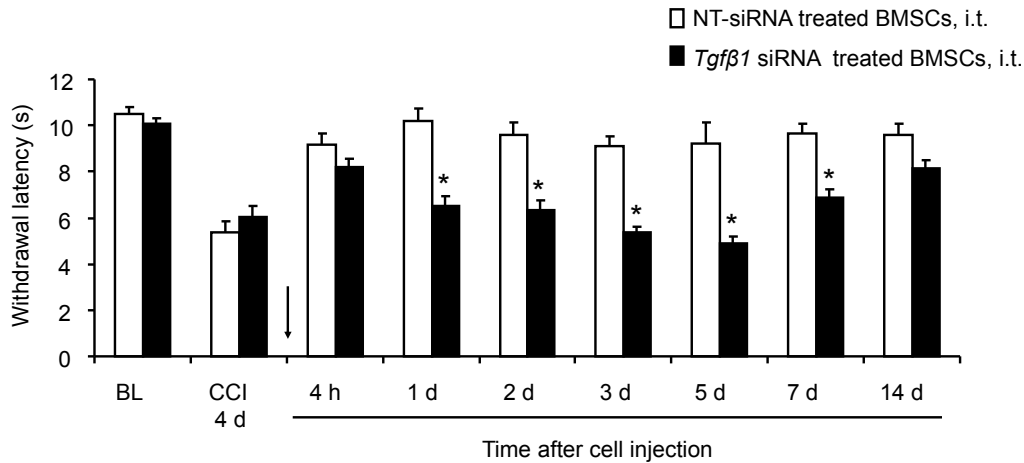
Supplemental Figure 1. Characterization of mouse BMSCs.

(A) Typical images of mouse BMSCs cultures at 1, 5 and 9 days in vitro (div) after plating. Initially, the cultured cells are mostly spindle-shaped with large round nuclei and a few thin cell processes (left); cells then became locally confluent, growing in distinct colonies at 5 days (middle) and approached confluence at 9 days (right). Scale, 20 μ m. (B-D) Flow cytometry analysis of cultured BMSCs at 9 days after plating. Up panels, SSC versus FSC scatter graphs. Low panels, plots of the number of immunoreactive cells versus relative fluorescence intensities. Note that 88% of the cultured BMSCs are positive for the stem cell marker CD90 (C) and only 2% of the cells are positive for the hematopoietic marker CD45 (D). Isotype-matched IgG-FITC antibody (B) was used as control.



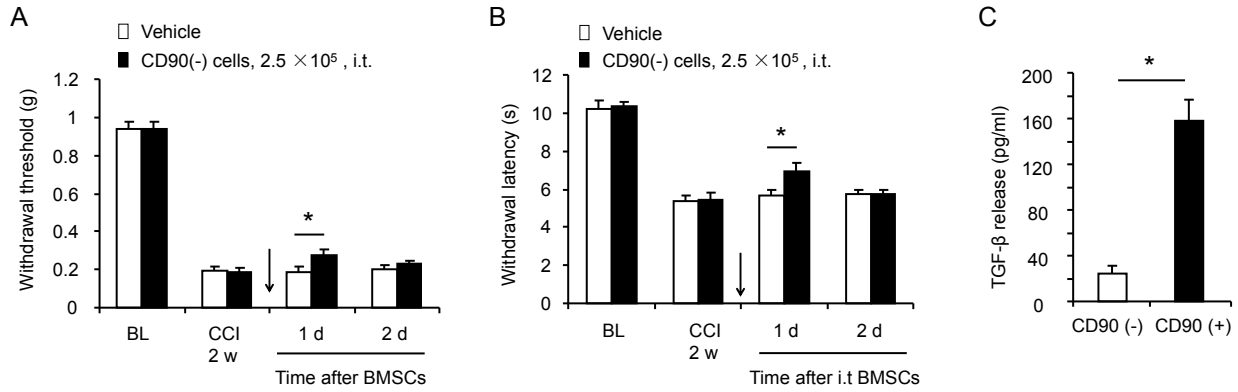
Supplemental Figure 2: The anti-allodynic and anti-hyperalgesic effects of intrathecal BMSCs (2.5×10^5) in earlier and later phases of CCI were reversed by the TGF-β1 neutralization.

(A-D) TGF-β neutralizing antibody (4 μg, i.t.), given at 1 day (A, B) or 24 days (C, D) after BMSCs injection, reverses BMSCs-induced inhibition of mechanical allodynia (A, C) and hyperalgesia (B, D) after CCI. n.s., no significance; * $P < 0.05$, compared with control IgG group; $n = 5-6$ mice per group. (E, F) TGF-β1 levels in CSF (E) and L5 DRGs (F) 28 days after BMSCs injection. * $P < 0.05$, compared with vehicle group. $n = 5-7$ mice per group. Statistical significance was determined by two-way ANOVA followed by Bonferroni post-hoc test (A-D) or Student's t test (E and F). All data are expressed as mean \pm S.E.M.



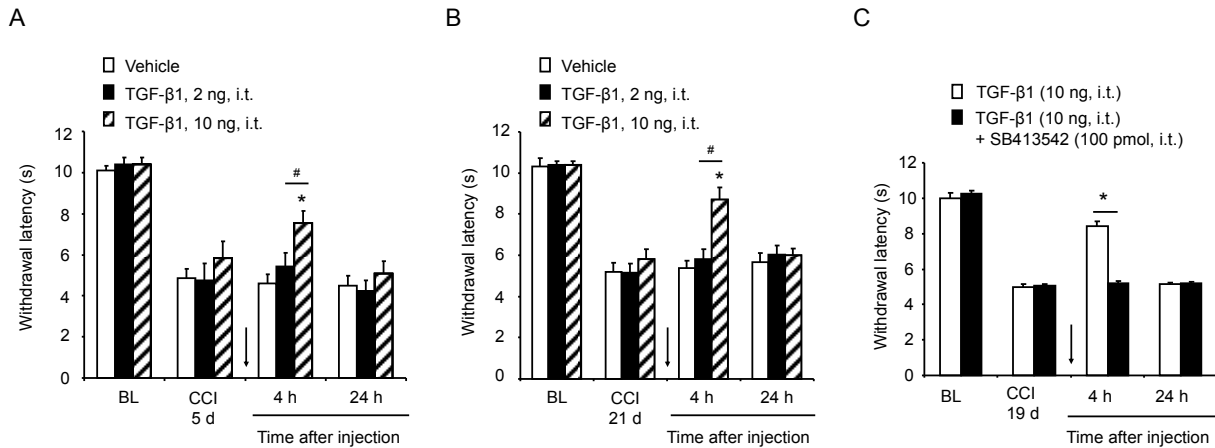
Supplemental Figure 3. Effects of BMSCs, pre-treated with *Tgfβ1* or control siRNA, on CCI-induced thermal hyperalgesia in CCI mice.

Intrathecal injection of non-targeting siRNA treated BMSCs (2.5×10^5) reversed thermal hyperalgesia for >14 d. However, this inhibitory effect was compromised when BMSCs were pre-treated with *Tgfβ1* siRNA. Arrow indicates the injection of BMSCs on CCI day 4. Note the difference between the two groups disappeared 2 weeks after the BMSCs injection. * $P < 0.05$, compared with non-targeting control siRNA treated group. $n = 5$ mice per group. Statistical significance was determined by Student's t test. Data are expressed as mean \pm S.E.M.



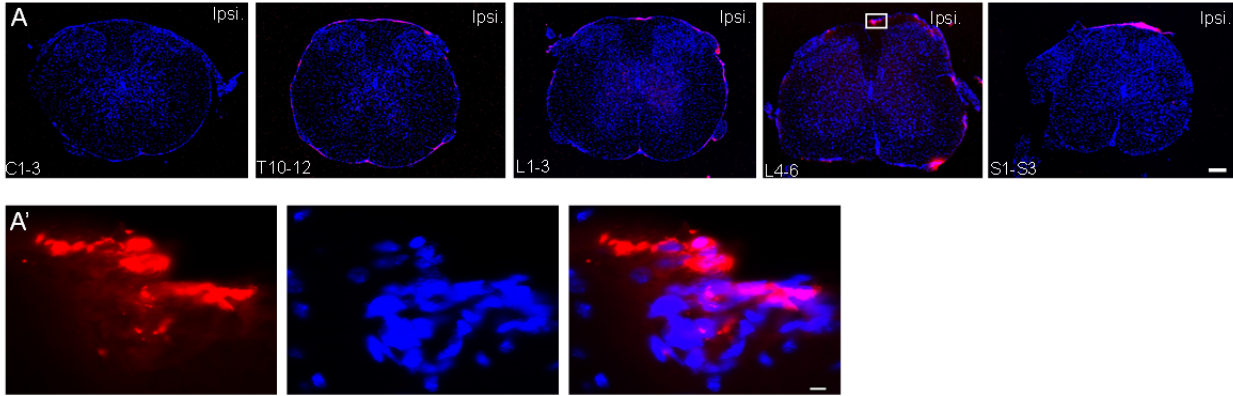
Supplemental Figure 4: Intrathecal injection of CD90-negative cells produced mild and transient relief of neuropathic pain after CCI.

(A, B) Intrathecal injection of CD90-negative cells, 2 weeks after CCI, only elicited mild and transient inhibition of CCI-induced mechanical allodynia (A) and heat hyperalgesia (B). * $P < 0.05$, compared with vehicle group; $n = 6$ mice/group. (C) ELISA analysis showing that CD90-negative cells secreted much less TGF- $\beta 1$, compared to CD90-positive cells. * $P < 0.05$, $n = 6$ mice/group. Statistical significance was determined by two-way ANOVA followed by Bonferroni post-hoc test (A and B) or Student's t test (C). All data are expressed as mean \pm S.E.M.



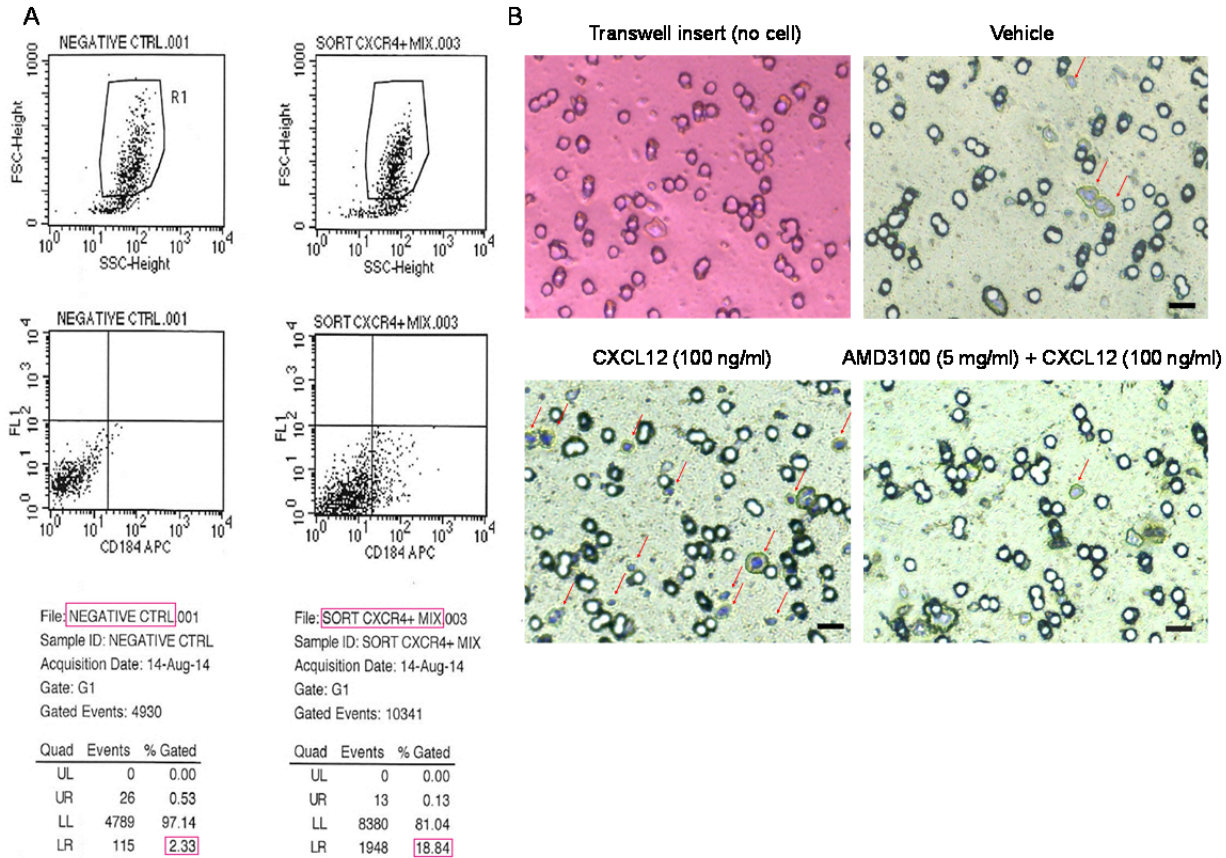
Supplemental Figure 5. TGF-β1 significantly attenuated CCI-induced thermal hyperalgesia through TGF-β receptor 1 (TGF-βR1).

(A, B) Intrathecal injection (indicated with an arrow) of TGF-β1 (2 and 10 ng) dose-dependently suppressed thermal hyperalgesia 5 and 21 days after CCI. $*P < 0.05$, compared with vehicle group; $^{\#}P < 0.05$; $n = 5$ mice per group. (C) Intrathecal injection (indicated with an arrow) of the TGF-βR1 inhibitor SB413542 (100 pmol) blocked the effect of TGF-β1 (10 ng) on thermal hyperalgesia. $*P < 0.05$, compared with TGF-β1 group; $n = 4$ mice for TGF-β1 group, $n = 5$ mice for TGF-β1 plus SB413542 group. Statistical significance was determined by Two-way repeated-measures ANOVA followed by Bonferroni post-hoc test (A, B) or Student's *t* test (C). All data are expressed as mean \pm S.E.M.



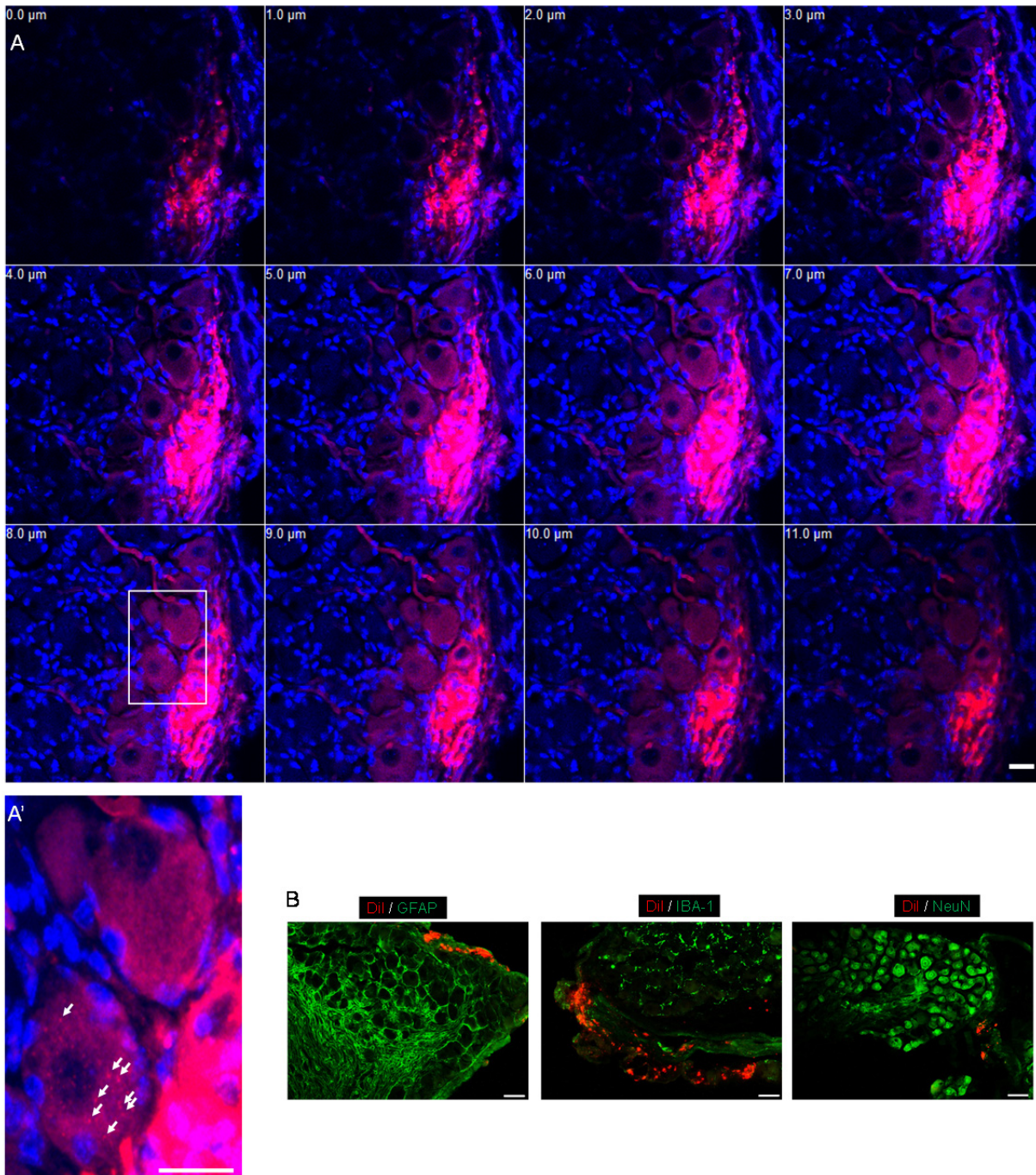
Supplemental Figure 6. Distribution of CM-Dil labeled BMSCs in spinal cord segments of CCI mice after intrathecal injection of Dil-labeled BMSCs.

(A) Dil-labeling on spinal cord sections from cervical (C), thoracic (T), lumbar (L), and sacral (S) segments of CCI mice receiving i.t. injection of CM-Dil-labeled BMSCs (2.5×10^5 , CCI-4 d). Animals were sacrificed 3 d after i.t. injection (7 d after CCI). Note a preferential accumulation of Dil-BMSCs on the edges of the spinal cord especially on the ipsilateral side. (A') Enlargement of the box in A for the staining of Dil (left), DAPI (middle), and merged (right). Scales, 200 μm in A and 20 μm in A'.



Supplemental Figure 7. CXCL12/CXCR4 axis controls the migration of BMSCs *in vitro*.

(A) Representative images of flow cytometric analysis showing surface expression of CXCR4 in BMSCs. Cells were stained with either specific anti-mouse CXCR4 antibody (right) or isotype-matched control antibody (left). The percentage of CXCR4⁺ BMSCs is 18.84%. It is possible that cells with low expression of CXCR4 were not detected. (B) Representative images of the transwell migratory assay. CXCL12 induced BMSCs migration, which was inhibited by CXCR4 antagonist AMD3100. Scale, 20 μ m.



Supplemental Figure 8. (A) Z-stack (1 μm interval) confocal images showing CM-Dil labeled BMSCs (2.5×10^5) in the L5-DRG 28 d after the i.t. injection. Note the close-proximity of BMSCs with DRG neurons. Scale, 20 μm . (A') Enlarged box in A. Arrows show the uptake of Dil-labeled particles by neurons adjacent to BMSCs, indicating active exchanges between neurons and BMSCs. Scale, 20 μm . Blue cells are DAPI-labeled nuclei. (B) Double staining of CM-Dil labeled BMSCs with GFAP (satellite glial marker), IBA-1 (macrophage marker), and NeuN (neuronal marker) in L5-DRGs 28 d after the i.t. injection of BMSCs. Note there is no co-localization with GFAP, IBA-1, and NeuN. Scales, 50 μm .